JOURNAL OF VIROLOGY, Aug. 2009, p. 7970–7981 Vol. 83, No. 16
0022-538X/09/$08.00+0 doi:10.1128/JVI.00521-09

Determinants of Hepatitis C Virus p7 Ion Channel Function and Drug Sensitivity Identified In Vitro▽

Corine StGelais,[1] Toshana L. Foster,[1] Mark Verow,[1,2] Elizabeth Atkins,[1] Colin W. G. Fishwick,[2] David Rowlands,[1] Mark Harris,[1] and Stephen Griffin[1]*

Institute of Molecular and Cellular Biology, Faculty of Biological Sciences and Astbury Centre for Structural Molecular Biology,[1] and School of Chemistry, University of Leeds, Leeds, West Yorkshire LS2 9JT, United Kingdom[2]

Received 13 March 2009/Accepted 28 May 2009

Hepatitis C virus (HCV) chronically infects 170 million individuals, causing severe liver disease. Although antiviral chemotherapy exists, the current regimen is ineffective in 50% of cases due to high levels of innate virus resistance. New, virus-specific therapies are forthcoming although their development has been slow and they are few in number, driving the search for new drug targets. The HCV p7 protein forms an ion channel in vitro and is critical for the secretion of infectious virus. p7 displays sensitivity to several classes of compounds, making it an attractive drug target. We recently demonstrated that p7 compound sensitivity varies according to viral genotype, yet little is known of the residues within p7 responsible for channel activity or drug interactions. Here, we have employed a liposome-based assay for p7 channel function to investigate the genetic basis for compound sensitivity. We demonstrate using chimeric p7 proteins that neither the two *trans*-membrane helices nor the p7 basic loop individually determines compound sensitivity. Using point mutation analysis, we identify amino acids important for channel function and demonstrate that null mutants exert a dominant negative effect over wild-type protein. We show that, of the three hydrophilic regions within the amino-terminal *trans*-membrane helix, only the conserved histidine at position 17 is important for genotype 1b p7 channel activity. Mutations predicted to play a structural role affect both channel function and oligomerization kinetics. Lastly, we identify a region at the p7 carboxy terminus which may act as a specific sensitivity determinant for the drug amantadine.

Hepatitis C virus (HCV) chronically infects 170 million individuals and is a major cause of severe liver disease such as cirrhosis and hepatocellular carcinoma. Acute HCV infection is asymptomatic which, combined with the lack of an available vaccine, means that the majority of carriers are unaware of their positive status. Thus, clinical intervention takes place upon the presentation of symptoms when liver damage is already extensive and when the virus is well established. Current therapy comprises a combination of pegylated alpha interferon (IFN-α) with ribavirin (Rib), which is effective in only 50% of cases and is both expensive and poorly tolerated by patients. This relatively low success rate is due to the highly prevalent, IFN-resistant genotype 1 viruses; other genotypes generally respond well to treatment (27). As IFN-Rib acts primarily via stimulation of the immune system, improving current therapy relies on the development of new, virus-specific drugs. A small number of polymerase and protease inhibitors are at late stages of development, but progress has been hampered by the inability until recently to culture HCV in vitro (21, 40, 45). The highly variable nature of HCV, however, means that new drugs will most likely have to be used in combination, making expansion of available drug targets and the development of new inhibitors a major research focus.

HCV is the prototype member of the *Hepacivirus* genus within the *Flaviviridae* (3). It is enveloped, and its genome is a 9.6-kb positive-sense RNA. This is translated in a cap-independent fashion from an internal ribosome entry site present within the 5′ untranslated region, yielding a 3,000-amino-acid polyprotein, which is cleaved by both cellular and viral proteases to generate 10 mature virus gene products: the structural proteins core and envelope E1 and E2, the p7 ion channel, and the nonstructural proteins NS2, NS3, NS4A, NS4B, NS5A, and NS5B which replicate the viral genome and regulate host cell metabolism (reviewed in reference 23).

The p7 ion channel of HCV is sensitive to several classes of inhibitor compounds in vitro (13, 26, 31) and is necessary for HCV to replicate in chimpanzees (32). Recently, p7 was shown to be critical for the secretion of infectious HCV particles in culture (19, 34), and we along with others have shown that drugs which block its activity significantly reduce virus production (12, 35). p7, therefore, represents an important new target for drug development, and clinical trials combining IFN and Rib with a p7 inhibitor, amantadine, have demonstrated improved response rates in genotype 1-infected individuals (6). Recently, we have shown that the sensitivity of HCV to p7 inhibitors varies according to genotype, implying that p7 sequence determines the binding of inhibitor compounds (12). Little is known about how primary sequence governs p7 channel activity or drug interactions although several mutations have been shown to affect particle secretion in culture (19, 34), including the conserved basic charges on the cytosolic loop, which are known to be required for p7 activity in surrogate cell systems (14).

p7 channels are heptameric assemblages (4) with a predicted

* Corresponding author. Mailing address: Institute of Molecular and Cellular Biology, University of Leeds, Garstang South, Mount Preston Street, Leeds, West Yorkshire LS2 9JT, United Kingdom. Phone: (44) 113 3433154. Fax: (44) 113 3435638. E-mail: s.d.c.griffin@leeds.ac.uk.

▽ Published ahead of print on 3 June 2009.

structure whereby the lumen is formed by the amphipathic amino-terminal *trans*-membrane helices (13, 25). Carboxy-terminal helices are thought to interact with adjacent p7 protomers, serving to stabilize the channel structure. In addition, the basic loop may form a constriction at one end of the channel, possibly serving to mediate channel gating (13). Accordingly, residues within the loop or the amino-terminal helix would be the most likely to mediate channel opening and/or drug binding.

Here, we have investigated determinants of both p7 drug sensitivity and channel activity using a liposome-based fluorescent dye release assay for p7 function (36). Surprisingly, we find that p7 drug sensitivity is not, in fact, determined by either helix nor by the basic loop alone, implying that overall channel structure strongly influences drug binding. Several mutations specifically blocked fluorescent dye release from liposomes without adversely affecting oligomerization or membrane insertion, validating the system as a convenient means of investigating p7 function. Lastly, we identify a region that influences resistance of genotype 1b p7 to amantadine. Developing our understanding of how p7 sequence is linked to drug sensitivity could have important implications for the design of future HCV therapies.

MATERIALS AND METHODS

DNA constructs. pGEX6P-1 (Pharmacia)-based bacterial expression constructs for FLAG-tagged J4 and JFH-1 p7 fused to glutathione-*S*-transferase have been described previously (4, 12). Chimeric J4/JFH-1 constructs and J4 p7 containing point mutations were generated by overlap/fusion PCR using appropriately designed primers (sequences available on request) and ligation of amplimers into pGEX6P-1 digested with EcoRI/NotI. All constructs were confirmed by double-stranded DNA sequencing.

Protein expression and purification. Glutathione *S*-transferase-FLAG-p7 proteins were expressed in *Escherichia coli*, purified from inclusion bodies, cleaved, and FLAG-p7 purified by reverse-phase high-performance liquid chromatography (HPLC) as previously described (4, 36). Protein molecular weights were confirmed by mass spectrometry.

Detection of recombinant p7. Western blot analysis of purified p7 was carried out as described previously (4, 36) using a commercial anti-FLAG mouse monoclonal antibody (M2; Sigma) or rabbit polyclonal serum raised to the carboxy terminus of J4 p7 (PPRAYA; no. 1055) (11), the JFH-1 p7 amino terminus (ALEKLVVLHAAS; no. 2715) (12), or JFH-1 p7 carboxy terminus (PRQAYA; no. 2717). Rabbit sera were peptide affinity purified, and both antibodies 2715 and 2717 were further concentrated ~50-fold by ammonium sulfate precipitation. Secondary antibodies conjugated to horseradish peroxidase were purchased from Sigma.

Native gel analysis of recombinant p7. Ten micrograms of lyophilized p7 from HPLC fractions was reconstituted in either 50 μM liposomes (see "Liposome dye release assay and drug inhibition studies" below) or 300 mM detergent (1,2-diheptanoyl-*sn*-glycero-3-phosphocholine [DHPC], dodecylphosphocholine [DPC], 1-myristoyl-2-hydroxy-*sn*-glycero-3-[phospho-RAC-(1-glycerol)] [LMPG], or 1-palmitoyl-2-hydroxy-*sn*-glycero-3-[phospho-RAC-(1-glycerol)] [LPPG]) and then adjusted to 150 mM Tris-Cl (pH 7.0), 30% glycerol, and 0.05% bromophenol blue prior to native polyacrylamide gel electrophoresis (PAGE) analysis on a 4 to 20% Tris-glycine gel (Invitrogen). Samples were not heated prior to analysis. Protein was visualized by staining with Coomassie brilliant blue.

CD of recombinant p7 in methanol. Circular dichroism (CD) spectra were collected at 1-nm intervals using a Jasco J175 spectropolarimeter (Jasco International Co., Ltd.) equipped with a Peltier thermostat, with a 1-mm path length quartz cuvette over the wavelength range of 190 to 260 nm. The protein samples were between 0.25 and 0.3 mg/ml in methanol. Values for methanol alone were subtracted for averaging and baseline correction.

Liposome flotation on discontinuous Ficoll gradients. Liposome flotations were carried out as previously described (36). Briefly, duplicate 90-μl batches of a protein-liposome mixture containing 5 μg of protein and 50 μM rhodamine-labeled liposomes were incubated at room temperature for 30 min. Ten microliters of assay buffer (36) or 1 M Na_2CO_3 (pH 11.4) was then added prior to a further 5-min incubation at room temperature. The mixture was then added to an equal volume of 40% Ficoll-assay buffer (wt/vol) and layered at the bottom of a 2.2-ml ultracentrifuge tube. This was then overlaid with 1.6 ml of 10% Ficoll-assay buffer (wt/vol) and then with 0.3 ml of assay buffer and spun at 100,000 × *g* for 1 h at room temperature. Gradients were fractionated, liposomes were detected by rhodamine fluorescence, and 20 μl from each fraction was subjected to Western blot analysis as described previously (36).

Liposome dye release assay and drug inhibition studies. Liposome dye release assays were performed as described previously (36). Assays are based on the real-time release of carboxyfluorescein from self-quenching concentrations within liposomes, resulting in dilution and subsequent fluorescence gain. Briefly, standard 100-μl assay mixtures contained 5 μg of purified protein dissolved in MeOH (giving ~5 μM final concentration) mixed with 50 μM carboxyfluorescein (CF)-liposomes (dioleoyl phosphatidic acid-phosphatidyl choline from Avanti polar lipids at 1:1 as described previously [36]). Inhibitors were added to reaction mixtures prior to temperature elevation. Baselines were determined using liposome-only and solvent controls (5% MeOH for addition of protein and/or 0.2% dimethyl sulfoxide for inhibitors). Release of CF was measured using a FLUOstar Optima plate reader (BMG Labtech) set to 37°C. Excitation and emission wavelengths were set at 485 nm and 520 nm, respectively. Fluorescence values were read every 30 s over a 30-min period in triplicate, with each experiment repeated at least twice on separate protein batches. Initial rates were calculated from the first 5 min of the reaction and expressed as change in relative fluorescent units per min (ΔRFU/min) as a percentage of the untreated control. The bee venom peptide mellitin (Sigma-Aldrich) at 10 nM and 1% Triton X-100 were used as positive controls for CF release. Amantadine-HCl was purchased from Sigma, and rimantadine-HCl was a kind gift from Helen Bright (formerly of GlaxoSmithKline, Stevenage, United Kingdom).

Molecular modeling of p7 ion channel complex. Models of the J4 p7 heptameric channel were constructed using Maestro (Schrödinger Inc.). Monomers were built amino acid by amino acid with energy minimization (magnetomotive force in a simulated water dielectric), docked into a heptameric structure, and then subjected to further energy minimization. Images of resultant structures were obtained by either Maestro or Pymol, version 0.9 (Delano Scientific).

RESULTS

Contribution of the p7 *trans*-membrane helices and loop regions to drug sensitivity. Recently, we found that p7 from different HCV isolates displayed discrete sensitivity patterns to inhibitors in vitro, which directly correlated with drug effects on particle secretion in culture (12). Models of the p7 channel structure heavily implicate the amino-terminal *trans*-membrane helix or the basic loop as sites for potential drug interactions as it is thought that their hydrophilic surfaces form the channel lumen (4, 13, 25). We reasoned, therefore, that chimeric proteins where these domains were exchanged would confer drug sensitivity relating to the genotype from which the amino-terminal helix/loop was derived.

To test this hypothesis, we constructed chimeric proteins using the J4 (genotype 1b) (43) and JFH-1 (genotype 2a) (20, 40) sequences as these display differential sensitivity to adamantane compounds: rimantadine blocks the activity of both proteins, whereas amantadine is only effective against J4 p7 (12). Importantly, both proteins are equally active in our dye release assay, and the chemistry of the two adamantane compounds is extremely similar. As both the helices and the cytosolic loops of J4 and JFH-1 differed in primary amino acid sequences, we generated a panel of four chimeric proteins (C1 to C4) (Fig. 1A). These combined the amino-terminal helix of one isolate with the carboxy-terminal helix of the other, in the context of either the J4 or JFH-1 cytosolic loop. Each protein was expressed to similar levels in bacteria, and purified chimeric p7 was confirmed by Western blotting using genotype-specific antibodies to the p7 amino or carboxy termini (Fig. 1A) (see Materials and Methods).

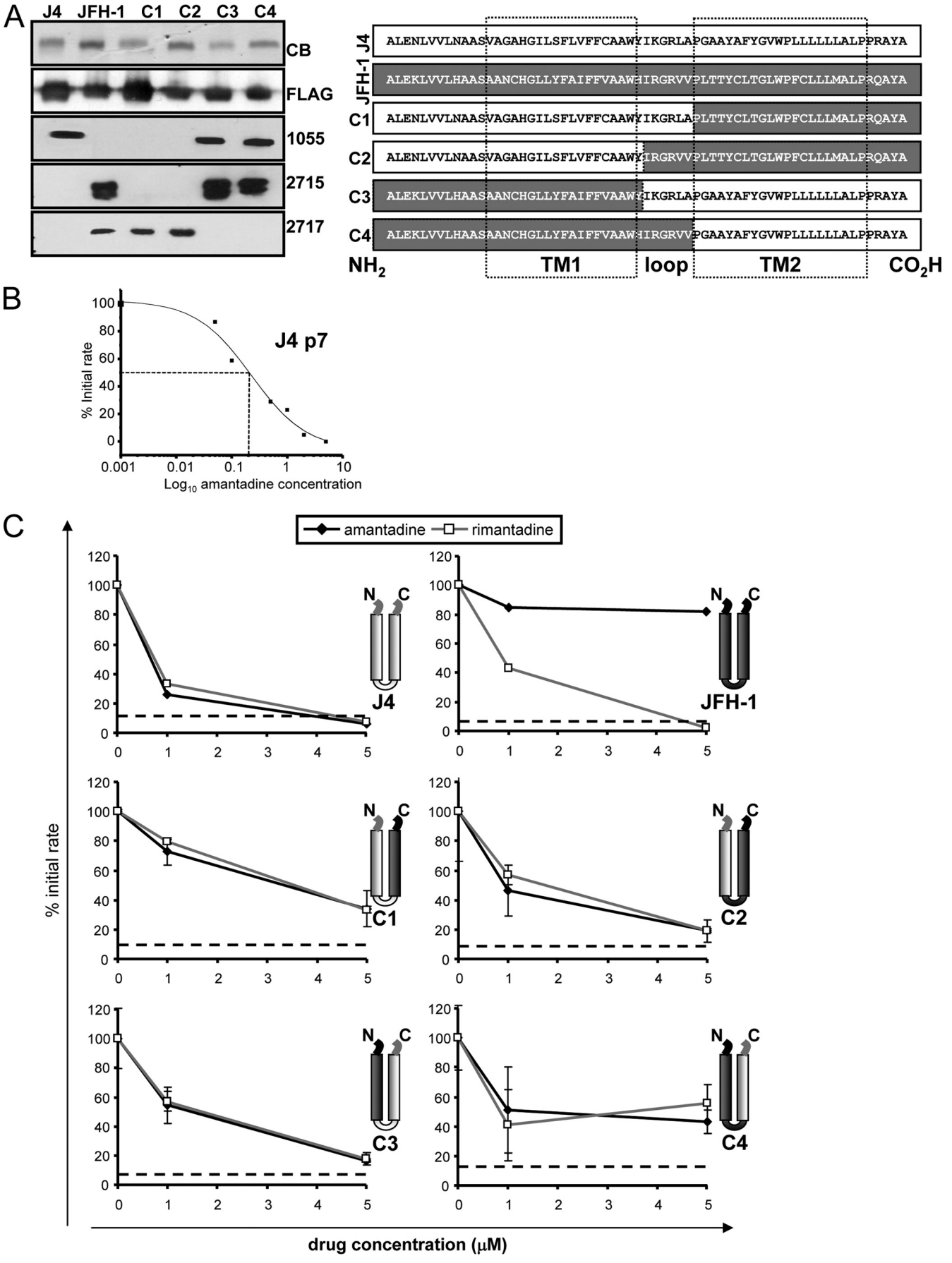
A
J4
JFH-1
C1
C2
C3
C4
CB
FLAG
1055
2715
2717
J4 ALENLVVLNAASVAGAHGILSFLVFFCAAWYIKGRLAPGAAYAFYGVWPLLLLLLALPPRAYA
JFH-1 ALEKLVVLHAASAANCHGLLYFAIFFVAAWHIRGRVVPLTTYCLTGLWPFCLLLMALPRQAYA
C1 ALENLVVLNAASVAGAHGILSFLVFFCAAWYIKGRLAPLTTYCLTGLWPFCLLLMALPRQAYA
C2 ALENLVVLNAASVAGAHGILSFLVFFCAAWYIRGRVVPLTTYCLTGLWPFCLLLMALPRQAYA
C3 ALEKLVVLHAASAANCHGLLYFAIFFVAAWYIKGRLAPGAAYAFYGVWPLLLLLLALPPRAYA
C4 ALEKLVVLHAASAANCHGLLYFAIFFVAAWHIRGRVVPGAAYAFYGVWPLLLLLLALPPRAYA
NH2
TM1
loop
TM2
CO2H
B
J4 p7
% Initial rate
Log10 amantadine concentration
C
amantadine
rimantadine
N
C
J4
JFH-1
C1
C2
C3
C4
% initial rate
drug concentration (μM)

The compound sensitivity of each chimera was then tested in a liposome-based fluorescent dye release assay, a convenient alternative to labor-intensive suspended bilayer systems (36) (Fig. 1C). Amantadine and rimantadine were used at 1 and 5 μM, based on the ability of amantadine to effect an ~80 and ~100% inhibition of the J4 protein at these concentrations (Fig. 1B). Chimeric proteins had reproducibly similar activities overall to parental proteins, as tested for at least three separate preparations of each (data not shown), but to accurately compare the inhibitory effects of increasing inhibitor concentration on each protein, activity is expressed as the percent initial rate of dye release compared to untreated samples in replicate experiments (Fig. 1C). Baseline levels of dye release were determined from solvent-only controls. As shown previously, J4 and JFH-1 p7 proteins displayed differential sensitivity to amantadine, with the JFH-1 protein remaining insensitive to the drug up to a 5 μM concentration (Fig. 1C, top panels) (12). Unexpectedly, chimeric proteins did not acquire the characteristics of one or other of the parental proteins and instead displayed intermediate sensitivity to both compounds (Fig. 1C, middle and bottom panels). While each chimera was more resistant to amantadine at 1 μM than J4 p7, the chimeras were also less sensitive to rimantadine than either parental protein. Improved inhibition was seen by increasing the drug concentration to 5 μM for all but the C4 chimera, which retained up to 50% activity in the presence of both compounds at this concentration. In addition, the C1 chimera showed increased resistance to both compounds present at 1 μM yet was strongly inhibited at higher drug concentrations. In each case, a degree of inhibition was seen for both compounds, as is the case for the J4 protein, yet no clear pattern emerged as to which elements were responsible for resistance to one or the other drug. Taken together, these data suggest that residues responsible for p7-drug interactions may act in a context-dependent fashion, dictated by the overall structure of the channel.

Design and expression of p7 point mutants in vitro. As data from chimeric proteins suggested that the contribution of individual residues within p7 may be context dependent, we designed a series of alanine substitutions targeting conserved residues in the J4 background thought to play a role in channel function and so, possibly, therefore drug interactions (Fig. 2A, top panel). The mutations fell into two categories: those changing charged/hydrophilic residues thought to line the channel lumen and those targeting residues predicted to affect channel stability. Within the first group, the most obvious targets were the basic charges on the cytosolic loop (K33A/R35A), which are required for channel activity in cells (14) as well as particle assembly (19, 34). We also changed three conserved hydrophilic residues within the amino-terminal helix, including a highly conserved histidine residue at position 17 (H17A, S21A, and C27A). Helical wheel models predict that these form one face of the amphipathic helix, thus lining the lumen of an oligomeric p7 channel (1, 4, 25). The second group of mutations comprised residues thought to stabilize the oligomeric channel structure: three phenylalanine residues in the amino-terminal helix (F22A/F25A/F26A) and a conserved glycine in the carboxy-terminal helix (G39A) thought to interact with adjacent protomers, a conserved proline predicted to form a "kink" in the carboxy-terminal helix (P49A), and, lastly, a leucine-rich region implicated in oligomerization (L50A to L55A [L(50-55)A]). All proteins were successfully expressed and purified from *E. coli*, verified using a J4-specific anti-p7 antibody (no. 1055) (see Materials and Methods) as well as the anti-FLAG monoclonal antibody (Fig. 2A). Western analysis revealed the sodium dodecyl sulfate (SDS)-induced formation of higher-molecular-weight forms of each protein as we have observed previously (Fig. 2A) (4).

The basic loop and a conserved histidine within the amino-terminal helix are required for p7 channel activity. We previously demonstrated that p7 is capable of functionally replacing the influenza A virus M2 protein in a surrogate cell system (14) and observed increased activity at lower pH for the J4 p7 protein in vitro (36). These observations strongly imply that p7 may act as a proton channel. In accordance with our findings in the M2 surrogate assay, mutation of the highly conserved basic charges on the cytosolic loop of J4 p7 resulted in a protein unable to mediate dye release from liposomes (Fig. 2B). Although a role for these residues in channel opening is likely, additional effects of this mutation are described in greater detail below.

The gating of M2 involves a conserved histidine at position 37, the protonation of which is critical for channel opening (30, 41). The p7 amino-terminal helix contains three hydrophilic residues (or clusters of residues in some isolates such as genotype 2a JFH-1), which are predicted to line the lumen and so are implicated in channel gating (Fig. 1 and 2). We mutated these residues to alanine in the J4 p7 sequence and tested the effect on channel opening in the liposome assay. Interestingly, of these, only the histidine mutation at position 17 caused a decrease in p7 channel activity (Fig. 2B). Neither of the other two hydrophilic residues (S21A or C27A mutations) had any effect on channel activity, nor did they alter susceptibility to amantadine (Table 1). This combined with our previous observations indicates that the pH-dependent mechanism governing the opening of p7 channels is similar to that of M2.

Mutations predicted to affect p7 stability affect both channel function and drug susceptibility. The hydrophobic interactions

FIG. 1. Drug sensitivity of chimeric J4/JFH-1 p7 proteins. Chimeric p7 proteins comprising J4 and JFH-1 amino and carboxy termini were expressed and purified from *E. coli* and assessed for their sensitivity to amantadine or rimantadine compared to the parental proteins. (A) Purified proteins were subjected to SDS-PAGE and Western analysis (left panel) using genotype-specific antibodies to J4 (no. 1055) or JFH-1 (no. 2717) carboxy termini or the JFH-1 amino terminus (no. 2715). Proteins were also probed with anti-FLAG monoclonal antibody and stained with Coomassie brilliant blue (CB). A schematic shows chimeric amino acid sequences for all four chimeras and parental proteins (right panel). White boxes, J4 sequence; black boxes, JFH-1 sequence. (B) A 50% inhibitory concentration curve for amantadine inhibition of J4 p7 in liposome CF release assays. (C) Liposome CF release assays for parental and chimeric proteins in the presence of increasing concentrations of amantadine or rimantadine. Activity is expressed as percent initial rate of untreated wild-type p7, measured by the ΔRFU/min for the first 5 min. The dotted line shows baseline dye release in solvent or liposome-only controls. Assays were performed for at least three separate batches of each protein with each condition in quadruplicate.

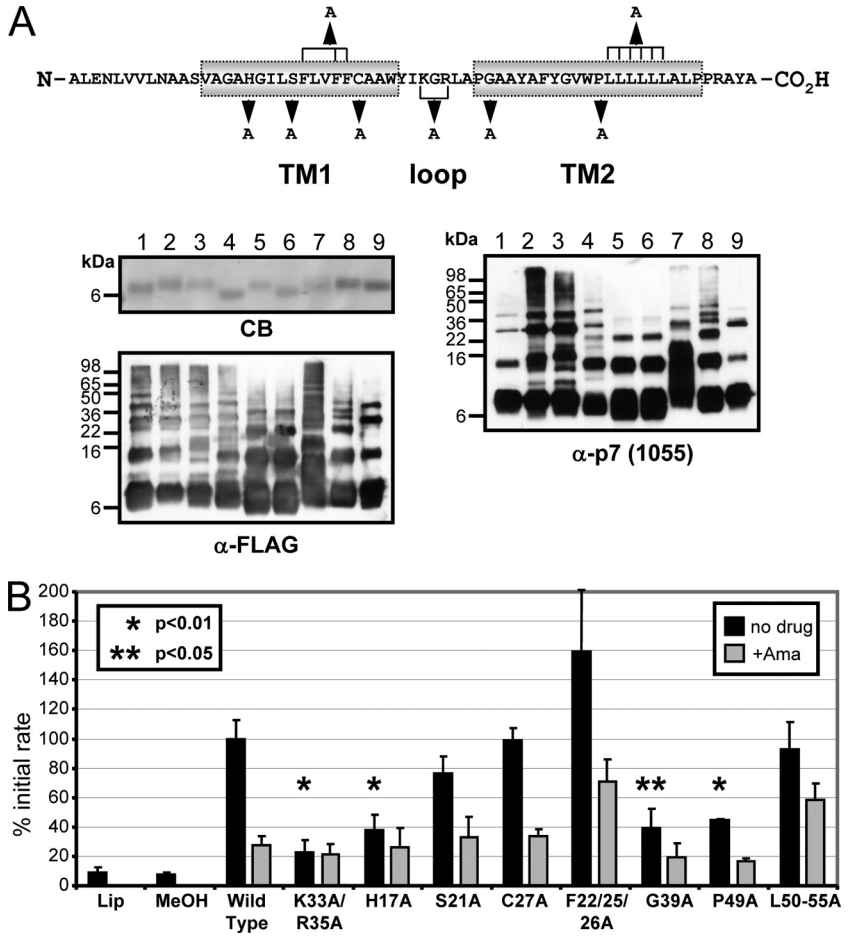

FIG. 2. Expression, purification, and activities of mutated J4 p7 proteins. (A) Key p7 residues were selected for alanine substitution mutagenesis as described in the Results section (top panel). HPLC-purified cleaved protein (5 μg) was then subjected to SDS-PAGE and Western blot analysis using an anti-FLAG monoclonal antibody and the J4-specific antibody (no. 1055) (bottom panels). Proteins were also stained with Coomassie brilliant blue (CB). Lanes 1, wild type J4 FLAG-p7; lanes 2, K33A/R35A; lanes 3, S21A; lanes 4, C27A; lanes 5, F22/25/26A; lanes 6, G39A; lanes 7, P49A; lanes 8, L(50-55)A; lanes 9, H17A. TM1 and TM2, *trans*-membrane helixes 1 and 2. (B) Activities of alanine substitution mutants of J4 p7 were assessed in the liposome dye release assay in the presence (+Ama) or absence (no drug) of amantadine (1 μM). Activity is expressed as the percent initial rate of untreated wild-type p7, measured by the ΔRFU/min for the first 5 min. Assays were performed for at least three separate batches of each protein with each condition in quadruplicate. Asterisks indicate *P* values generated from a Student *t* test where applicable. Baseline dye release values in solvent (MeOH) and liposome-only (Lip) controls are shown. α, anti.

TABLE 1. Summary of p7 mutant phenotypes

Protein	Activity[a]	Amantadine sensitivity	Phenotype
Wild type	+++	Yes	Wild type
K33A/R35A	−	NA[b]	Deficient membrane insertion
H17A	+/−	Yes	Strongly impaired activity
S21A	++	Yes	Mild reduction in activity
C27A	+++	Yes	Wild type
F22A/F25A/ F26A	+++++	Yes	Hyperactive channel
G39A	+/−	Yes	Strongly impaired activity
P49A	+/−	Yes	Concentration-dependent activity
L(50-55)A	+++	Reduced	Reduced inhibitor binding

[a] +++, 100%; ++, 80%; +, 60%; +/−, 40%; −,20%.
[b] NA, not available.

postulated to stabilize p7 oligomers were targeted by mutating key residues (Fig. 2A). One potential mechanism for p7 oligomerization is thought to proceed via the extended side chains of phenylalanine residues projecting into pockets in the hydrophobic surface of *trans*-membrane helices resulting from the small side chains of glycine residues (1). We therefore mutated three conserved phenylalanine residues in the p7 amino-terminal helix, as well as a conserved glycine in the carboxy-terminal helix, to alanine. Mutating the phenylalanine residues individually had no effect on channel activity in the liposome assay (data not shown); however, the triple mutation had the surprising effect of increasing p7-dependent dye release (Fig. 2B). This was reproducible for multiple protein preparations, yet no obvious increase in the amount of protein incorporated into liposomes was evident (data not shown), suggesting that the specific activity of the channel itself had been altered. In contrast, the G39A mutation significantly reduced p7 channel ac-

tivity. Interestingly, neither of these mutations affected the ability of p7 to form higher-molecular-weight structures in the presence of SDS (Fig. 2A).

An additional level of stability may be conferred to p7 channel structures by a predicted kink in the carboxy-terminal helix caused by a highly conserved proline residue at position 49. This kink is thought to allow the carboxy terminus of the helix to bend around adjacent monomers and form close-knit hydrophobic interactions (13, 25). The precise type of interaction this brings about is unknown although many HCV isolates possess a leucine-rich region toward the end of the carboxy-terminal helix which may act as a hydrophobic "zipper," as increasingly documented for oligomeric channel proteins (8, 44). We therefore mutated both motifs and assessed their effects on channel activity. Surprisingly, whereas the P49A markedly reduced channel activity, the L(50-55)A mutation retained wild-type activity yet showed an increased resistance to 1 μM amantadine (Fig. 2B).

Impaired mutant channel activity is not due to defects in protein folding or oligomerization. It was necessary to demonstrate that the effects of the alanine substitutions with impaired activity were due to the formation of inactive channels rather than an inability of the protein to fold or self-associate. Although SDS-PAGE "laddering" correlates well with the formation of heptameric complexes induced by SDS in solution (4), the denaturing aspects of SDS-PAGE (SDS itself along with heating of the sample) disrupt channel complexes to a degree, thereby reducing the amount of resolvable heptameric species (Fig. 2A). We therefore tested a number of less-denaturing detergents for their ability to induce the formation of p7 oligomers by native PAGE (Fig. 3A, left-hand panel). We found that the phospholipid-like DHPC and DPC were capable of inducing the formation of heptameric J4 FLAG-p7 complexes, whereas neither LMPG nor LPPG did so. Equivalent assemblages were observed when protein was mixed with liposomes, as described for the dye release assay (Fig. 3A, middle panel), making it likely that these species represented a relevant oligomeric form of the channel. Reconstitution of null mutants in DHPC also resulted in heptameric complexes (Fig. 3A, right-hand panel) although the K33A/R35A mutant protein gave a less-well-defined smear, raising the possibility of some heterogeneity or a less efficient self-association.

In addition to their ability to oligomerize, the secondary structure of mutant proteins was also assessed by CD (Fig. 3B). Results are shown for protein dissolved in methanol; this was deemed valid as protein solubilized in this way is functional in liposome dye release assays and so presumably is correctly folded or is, at the very least, in a conformation capable of assuming a native structure upon lipid/detergent incorporation. Indeed, wild-type J4 p7 protein reconstituted in liposomes or DHPC gave identical profiles (data not shown). All mutated proteins gave the same alpha-helical profile as seen for wild-type p7, indicating that no gross defects in secondary structure had arisen.

Dominant negative effects of basic loop and H17A mutants support preassembly of channel complexes prior to membrane insertion in vitro. Given that all mutated p7 proteins were correctly folded and could oligomerize in DHPC, we next assessed whether their ability to associate with membranes was intact. Protein-liposome mixes were subjected to flotation on a discontinuous Ficoll gradient in the presence or absence of a high-pH wash to strip nonintegrated protein. Fractions were tested for liposome content by rhodamine fluorescence, which indicated that liposomes had migrated to the 10% Ficoll-aqueous interface (Fig. 4A, fraction 11). The presence of high pH did not affect liposome flotation (Fig. 4A, histogram in right-hand panel). Fractions were subjected to Western blotting to assess the amount of liposome-associated protein. As seen previously, a significant proportion of the wild-type J4 p7 associated with liposomes (36). Furthermore, this association was resistant to high pH, indicating that the protein had fully inserted into the liposome membrane. This was also true for p7 mutants with the exception of the K33A/R35A mutant protein, which dissociated from the liposomes following high-pH treatment. This mutation represents the most severe change to the overall charge/hydrophobicity of p7, making this observation perhaps unsurprising. It does, however, make it impossible to assign a role for this conserved motif in channel opening using this system.

We next asked whether inactive mutant proteins could exert a dominant negative effect over wild-type p7 function via the formation of nonfunctional mosaic channels. As this phenotype should manifest if even one protomer of a heptameric channel structure contained the mutation, we performed liposome assays titrating mutant proteins into a wild-type reaction mixture at increments of one-seventh of the total protein content and compared activity to the equivalent amount of wild-type protein alone. We tested both the K33A/R35A and H17A mutants to assess whether any effect could occur in the absence of membrane insertion. Surprisingly, both mutant proteins were able to reduce wild-type dye release activity to nearly baseline levels even when present at only one-seventh of the total protein concentration (Fig. 4B). As the K33A/R35A mutant exerted the same effect as the H17A protein, this strongly supports the idea that, at least in this system, p7 oligomers form at the membrane surface prior to the insertion of intact channel complexes (Fig. 4A).

Titration of p7-null mutants reveals a key role for conserved proline 49 in channel oligomerization. It was important to demonstrate that the null phenotypes of mutants were not due to concentration-dependent effects. We therefore performed titration experiments with protein inputs from 20 to 200% (1 to 10 μg of protein) of that in a standard reaction mixture (5 μg) and measured activity relative to the wild type. Importantly, liposomes were still present in excess where 10 μg of protein was used since dye release for wild-type p7 did not exceed 40% of either mellitin- or Triton X-100-positive controls (data not shown).

For the K33A/R35A mutant, no activity was observed even at 200% input, implying that this protein is totally incapable of membrane insertion. For the G39A mutation, again no increase in activity was observed over the lowest input, indicating that this mutant protein formed truly nonfunctional channels (Fig. 5A). For the H17A mutant, however, a modest increase in CF release was observed with increasing concentration (Fig. 5A) although this difference was not statistically significant compared to standard reaction conditions.

Unlike the other mutations, the P49A mutation displayed a concentration-dependent switch in activity, shifting from 40% activity under standard conditions to almost threefold wild-type activity at 150% and 200% input (Fig. 5A). To investigate the cause of this switch, we subjected protein from P49A and G39A

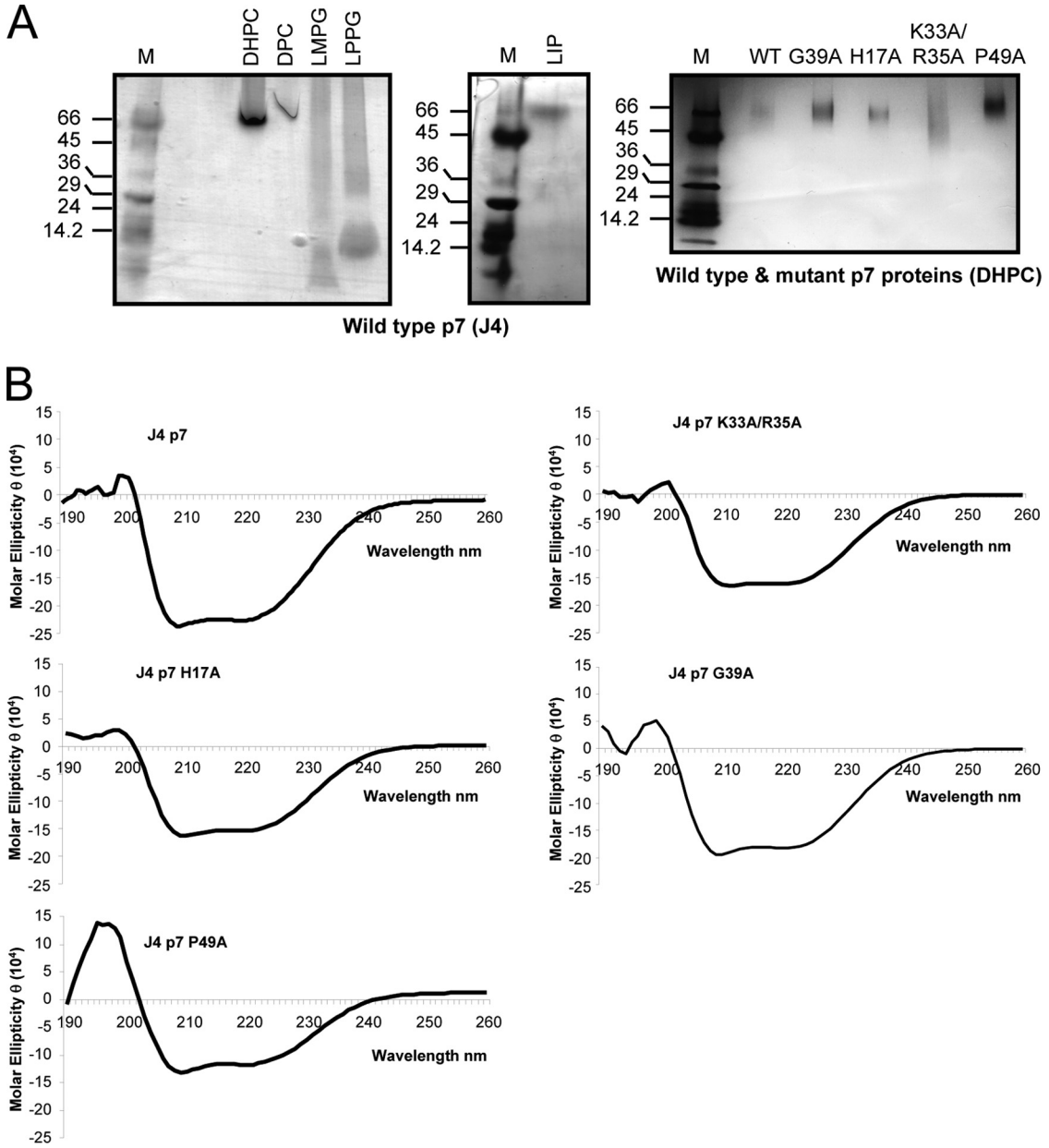

FIG. 3. Oligomerization and folding of p7 null mutant proteins. (A) Mild detergents were tested for their ability to induce oligomerization of wild-type J4 FLAG-p7 during native PAGE. Both DHPC and DPC (300 mM) induced heptamer formation, whereas LMPG and LPPG did not (left panel). Wild-type protein was mixed with 50 μM liposomes (LIP) and analyzed by native PAGE (middle). Null-mutant p7 proteins were reconstituted in 300 mM DHPC, and oligomeric forms were resolved by native PAGE (right). (B) Wild-type and null-mutant proteins dissolved in methanol were assessed for alpha-helical content using CD. WT, wild type; M, molecular mass markers (kDa).

titration experiments to SDS-PAGE and Western analysis to visualize oligomeric forms under partially denaturing conditions (Fig. 5B). In agreement with the sudden switch in activity for the P49A mutant, a marked increase in the amount of higher-molecular-weight species was observed upon increasing protein input from 5 to 7.5 μg (Fig. 5B, right panel). This was not observed for either the wild-type or G39A mutant proteins (Fig. 5B, left and central panels), implying that Pro 49 may serve to regulate efficient oligomerization of p7 channel complexes.

A carboxy-terminal polyleucine motif contributes to amantadine sensitivity of genotype 1b p7. As described above, the L(50-55)A mutation appeared to display increased resistance to treatment with 1 μM amantadine. To determine whether this effect was specific, we tested this protein in drug titration assays against increasing concentrations of both amantadine and rimantadine (Fig. 6). While this mutation conferred resistance to 1 μM amantadine, increasing the drug concentration effectively blocked its activity, whereas the protein was equally sensitive to both low and high concentrations of rimantadine (Fig. 6). This pattern of drug sensitivity is reminiscent of the JFH-1 protein (Fig. 1 and 6), albeit to a much lesser degree as higher amantadine

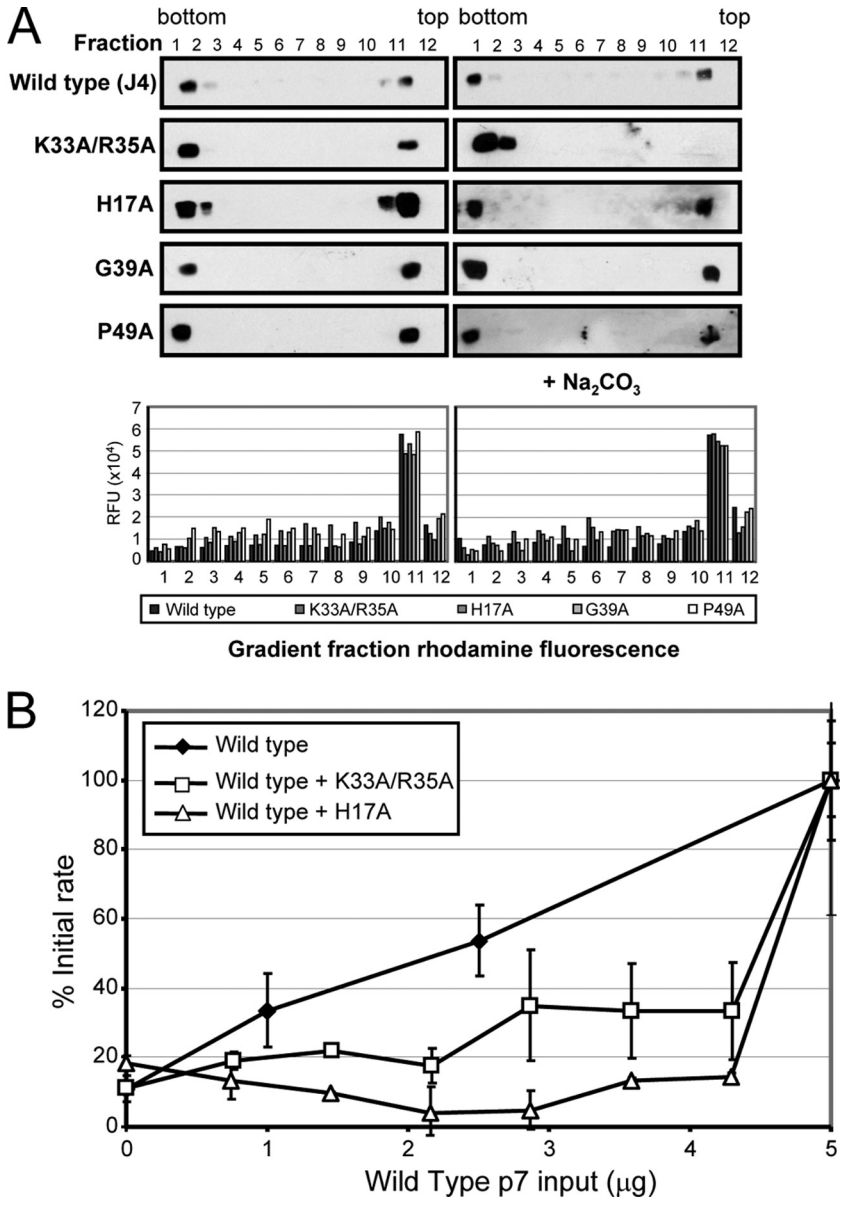

FIG. 4. Membrane association and dominant negative effects of mutant J4 p7 proteins. (A) p7-null mutations were assessed for membrane association in the presence or absence of high pH (100 mM Na_2CO_3 [pH 11.4]). Anti-FLAG Western blots from fractionated discontinuous Ficoll gradients are shown from 1 (bottom) to 12 (top). Bottom panels show rhodamine fluorescence of gradient fractions with liposomes floating to the 10% Ficoll-aqueous interface (fraction 11). (B) Basic loop K33A/R35A and H17A mutant proteins were tested for their ability to exert a dominant negative effect over wild-type protein by mixing in increments of one-seventh of the total 5 μg of input compared to the corresponding amount of wild-type protein alone and testing resultant channel activity in the liposome dye release assay. Activity is expressed as the percent initial rate of untreated wild-type p7, measured by the ΔRFU/min for the first 5 min.

concentrations effectively block activity. This may be evidence that p7 possesses distinct sensitivity determinants for these two related compounds or that rimantadine binds with much higher affinity than amantadine.

DISCUSSION

This study represents the first mutagenic analysis of the HCV p7 ion channel in vitro. It sought to identify determinants of both ion channel function and drug sensitivity based on previous homology searches and structural predictions.

Our recent finding that the sensitivity of HCV to p7 inhibitors is genotype dependent (12) prompted us to construct chimeras between the amantadine/rimantadine-sensitive J4 and the amantadine-resistant/rimantadine-sensitive JFH-1 p7 sequence. Contrary to expectation, drug sensitivity was not dictated by the amino-terminal *trans*-membrane domain, which is predicted to line the pore of the p7 channel complex (4, 13, 25). Chimeric proteins displayed intermediate drug sensitivi-

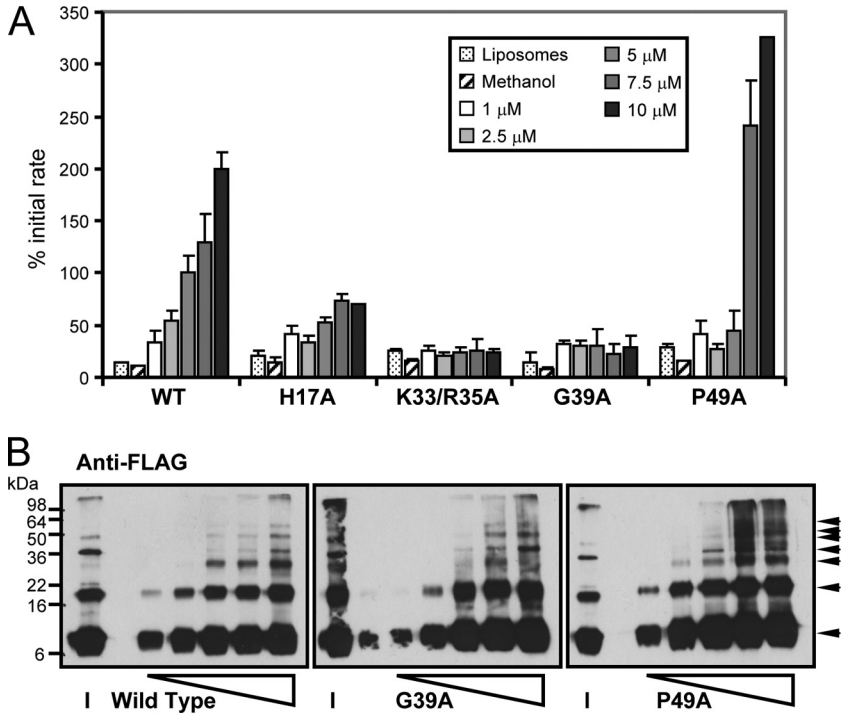

FIG. 5. Effect of protein concentration on p7-null mutant dye release. Increasing amounts of null-mutant proteins were titrated into the dye release assay from 20 to 200% standard input levels. (A) Channel activity is expressed as the percent untreated wild-type (WT) protein initial rate under standard conditions (100% is equivalent to 5 μg in 100 μl, giving a final concentration of ~5 μM). (B) Western blot analysis of wild-type, G39A, and P49A proteins taken following titration experiments showing higher-molecular-mass oligomeric forms of p7 in SDS micelles (arrows). One-tenth of the total amounts of protein used in the experiment described in panel A was loaded.

ties relative to the parental sequence (Fig. 1C), indicating that residues conferring drug sensitivity must do so within the context of the overall channel structure. It is notable that considerable variation in pore-lining hydrophilic clusters within the amino-terminal helix exists between genotypes and often coincides with similar variation in the carboxy-terminal helix. This is well illustrated in Fig. 1, with JFH-1 p7 having additional hydrophilic residues in both helices compared with J4.

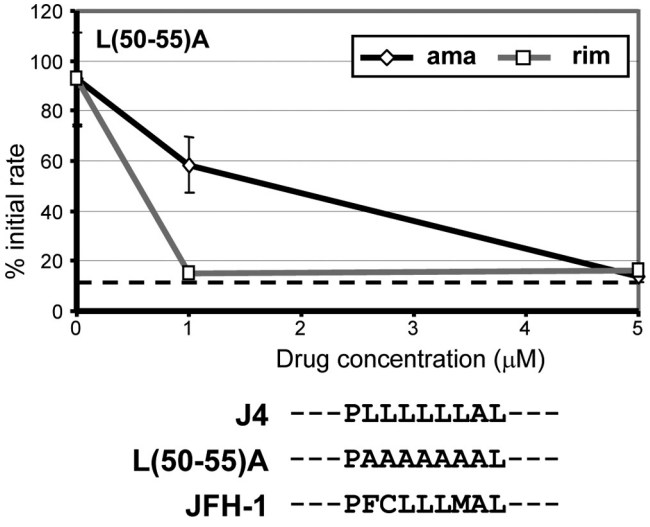

FIG. 6. Decreased sensitivity of a polyleucine mutation L(50-55)A to low concentrations of amantadine but not rimantadine. Polyleucine mutant protein was subjected to 1 or 5 μM rimantadine (rim) or amantadine (ama), and channel activity was assessed in liposome dye release assays. The lower panel shows a comparison of amino acids in the carboxy terminus for J4, the L(50-55)A mutant, and JFH-1 1 proteins.

We next analyzed a series of alanine substitutions in the background of the genotype 1b J4 p7 protein. None of the mutations altered the secondary structure of p7 or its ability to oligomerize under native conditions (Fig. 3A and B). Consistent with our previous observations (4), FLAG-p7 (~9 kDa) channel complexes appeared heptameric in nature (~63 kDa) by native PAGE in the presence of both liposomes and membrane-mimetic detergent molecules (Fig. 3A). Unlike our previous SDS-PAGE methodology, no intermediate species were apparent when heptamers were formed, suggesting that this complex is energetically stable and likely represents the native channel structure in vivo.

Mutation of the dibasic K33-R35 motif to alanine abrogated channel activity in liposomes. Similar mutations block HCV particle production in culture (19, 34) and replication in chimpanzees (32), as well as p7 activity in surrogate cellular assays (14). Analogous mutations also block production of infectious bovine viral diarrhea virus in culture (15) as well as replication of GB virus B in tamarins (38). Interestingly, our analysis indicates that this mutant protein is unable to insert into membranes although it can associate with them (Fig. 4A), which is consistent with this region's being part of a putative membrane insertion motif in vitro (28). Furthermore, this mutant protein was able to exert a dominant negative effect on wild-type channel activity (Fig. 4B), indicating that p7 channels may assemble

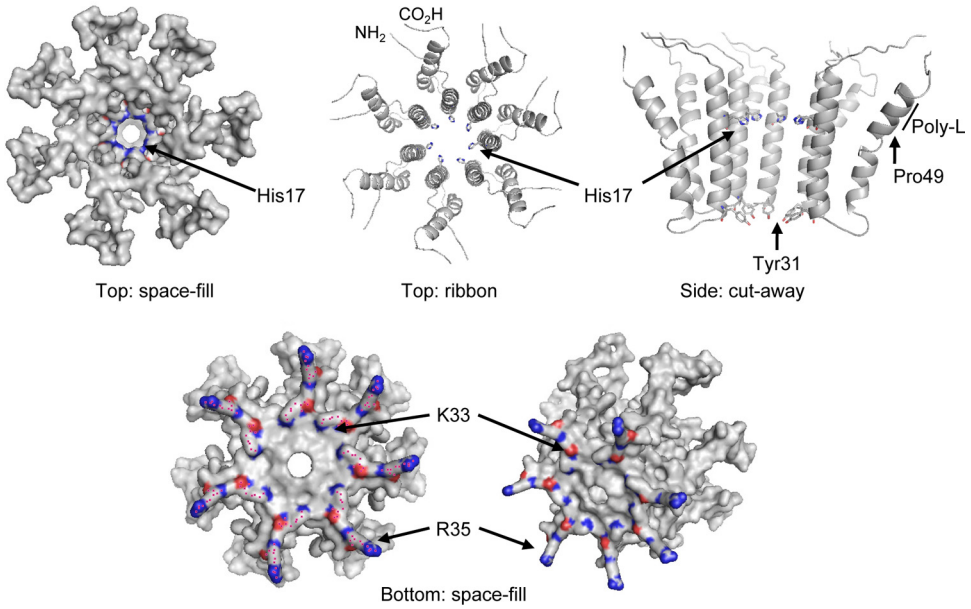

FIG. 7. Molecular modeling of the J4 p7 ion channel complex. J4 p7 protomers were modeled with free energy minimization using the Maestro program and then manually docked into a symmetrical heptameric complex. The top panel shows top-down views and a side projection (two protomers removed) of channel complexes with the potential pH sensor, His 17, and possible gate, Tyr 31, highlighted. In addition, the positions of Pro 49 and Leu 50 to Leu 55(Poly-L) are indicated on the side projection to illustrate the interactions with adjacent protomers. Last, bottom views of the complex are shown, illustrating the apposed basic residues of the cytosolic loop, which may promote the hairpin conformation of each protomer.

on the membrane surface prior to insertion. In cells, however, membrane insertion would depend on the signal recognition particle although conserved basic charges are known to be critical components of HCV *trans*-membrane proteins and are required for correct localization and folding(5). Consistent with this, we have found that the equivalent mutation in cell culture causes pronounced disruption of E2-p7-NS2 processing (S. Griffin, unpublished data).

Unlike the basic loop mutation, the H17A mutant was able to insert into membranes yet remained defective for channel function. His 17 is located within the amino-terminal *trans*-membrane domain and was recently shown to line the channel lumen by Cu^{2+}-mediated inhibition of channel activity (2). Similar inhibition is observed for His 37 of the influenza virus M2 channel (10), which we have shown to share functional similarity with p7 (14). This is strongly suggestive that p7 channel opening also depends on protonation of His 17, yet in the aforementioned study a genotype 1a H77 H17A mutant protein remained functional. This counter-intuitive finding may indicate that hydrophilic residues within the *trans*-membrane domains of all p7 sequences are often present as pore-lining clusters. It is therefore likely that the functionality of individual amino acids may be influenced by adjacent residues. In the J4 sequence His 17 exists in isolation, whereas for H77, His 17 is part of a cluster together with Thr 16. Logically, mutating this residue alone is more likely to affect J4 p7 channel function than H77. Accordingly, for JFH-1 p7 which contains the cluster Asp 15-Cys 16-His 17, an H17A mutation alone does not block particle production in culture (S. Griffin, unpublished). His 17, however, is highly conserved among p7 sequences, and our observation that mutating other hydrophilic residues within the J4 amino-terminal helix had no consequence for channel activity (Fig. 2B) emphasizes its likely importance for channel opening.

A recent report suggested that p7 may utilize an HXXX(Y/W) gating motif (22), reminiscent of the HXXXW motif found in influenza M2 where protonation of His 37 results in a conformational change in Trp 41, resulting in channel opening (24, 30, 39). Unfortunately, mutation of either His 17 or Tyr 21 in the context of JFH-1 p7 resulted in little effect on HCV particle production, and the motif is only partially conserved among HCV isolates. Given the heterogeneity of the hydrophilic clusters within p7 sequences, however, it is conceivable that their associated gating residues also vary in position and nature. Determination of high-resolution structural information will be required to define the interactions that may occur between a putative p7 proton sensor and corresponding aromatic gating residues.

Of the mutations predicted to affect channel stability, both G39A and P49A caused a specific ion channel defect under standard conditions (Fig. 2B), yet titration of increasing amounts of protein revealed a sudden switch of P49A protein to a hyperactive channel compared with the wild-type protein (Fig. 5A). This correlated with the increased formation of oligomeric complexes under partially denaturing conditions (visualized by SDS-PAGE laddering) (Fig. 5B), suggesting that Pro 49 may regulate the formation of channel complexes. This is reminiscent of a growing number of membrane-active peptides, whose activity is governed by proline *cis*/*trans* isomerization (9, 18, 42). Pro 49 is predicted to form a kink in the carboxy-terminal *trans*-membrane domain, the orientation of which could conceivably regulate the formation of a stable heptamer. This could provide a means of regulating channel activity within separate subcellular compartments and may be

linked to the observation that p7 has been shown to display both discrete subcellular localization and membrane topology within cells (11, 16).

We expected that mutation of the polyleucine motif at the p7 carboxy terminus might disrupt oligomerization as leucine zippers are thought to stabilize some channel complexes, including human immunodeficiency virus type 1 Vpr (8). The L(50-55)A mutant protein displayed essentially wild-type characteristics yet showed differential sensitivity to amantadine and rimantadine, reminiscent of the JFH-1 p7 protein (Fig. 6). The corresponding amino acid sequence in JFH-1 is markedly less hydrophobic than the J4 sequence (Fig. 6). Interestingly, whereas inhibition of M2 channels by these drugs has historically been associated with their binding to residues within the channel lumen in a "bottle-stopper" fashion (7, 37), a recent nuclear magnetic resonance study located rimantadine binding to the outside of the channel stabilizing its closed conformation (33) although this is highly controversial (17). Logically, variation in hydrophobicity might be expected to affect drug binding, and some influenza amantadine escape variants have mutations affecting this region. Given that the polyleucine region is predicted to lie on the outside of the p7 channel, variation in this region may partially explain genotype-dependent drug sensitivity. Further mutagenesis studies are ongoing to map precise determinants of p7 inhibitor susceptibility.

To set the effects of p7 mutations in context, we undertook molecular modeling of the J4 p7 ion channel complex using the Maestro program (Fig. 7). The energy-minimized model of a heptameric complex largely supported observations from dye release assays. Importantly, His 17 from each monomer was predicted to line the channel lumen following energy minimization, consistent with Cu^{2+} binding (2), its functional importance and potential role as a pH sensor (Fig. 7). In turn, Tyr 31 was predicted to constrict the aperture on the cytosolic side of the channel, implying that it may play a role as the gating residue associated with His 17. The basic Lys 33 and Arg 35 loop residues repelled each other, possibly serving to stabilize the hairpin conformation of each protomer (Fig. 7). As predicted, the polyleucine motif was found to interact with the amino-terminal helix of adjacent protomers, facilitated in part by the flexibility of Pro 49. Interestingly, recent studies of amantadine binding to M2 cite destabilization of channel complexes as a possible mechanism underlying drug resistance, thus reducing hydrophobic drug-protein interactions (29). The L(50-55)A mutant, therefore, may bind the less-hydrophobic amantadine less avidly than rimantadine, which is rendered more hydrophobic by its additional methyl group.

This work represents the first step toward defining how primary sequence determines HCV p7 channel opening and drug sensitivity. Understanding these processes is vital to the development of p7 as a target for much needed future HCV therapies.

ACKNOWLEDGMENTS

We thank Andrew Macdonald (University of Leeds) for critical reading of the manuscript and useful discussion.

C.S. and E.A. received Cooperative Awards in Science and Engineering Ph.D. studentships from the Biotechnology and Biological Sciences Research Council and Pfizer. T.F. is funded by a Wellcome Trust Ph.D. studentship. S.G. is the recipient of a Medical Research Council New Investigator Award (G0700124).

REFERENCES

1. **Carrere-Kremer, S., C. Montpellier-Pala, L. Cocquerel, C. Wychowski, F. Penin, and J. Dubuisson.** 2002. Subcellular localization and topology of the p7 polypeptide of hepatitis C virus. J. Virol. **76:**3720–3730.
2. **Chew, C. F., R. Vijayan, J. Chang, N. Zitzmann, and P. C. Biggin.** 2009. Determination of pore-lining residues in the hepatitis C virus p7 protein. Biophys. J. **96:**L10–L12.
3. **Choo, Q. L., G. Kuo, A. J. Weiner, L. R. Overby, D. W. Bradley, and M. Houghton.** 1989. Isolation of a cDNA clone derived from a blood-borne non-A, non-B viral hepatitis genome. Science **244:**359–362.
4. **Clarke, D., S. Griffin, L. Beales, C. S. Gelais, S. Burgess, M. Harris, and D. Rowlands.** 2006. Evidence for the formation of a heptameric ion channel complex by the hepatitis C virus p7 protein in vitro. J. Biol. Chem. **281:**37057–37068.
5. **Cocquerel, L., C. Wychowski, F. Minner, F. Penin, and J. Dubuisson.** 2000. Charged residues in the transmembrane domains of hepatitis C virus glycoproteins play a major role in the processing, subcellular localization, and assembly of these envelope proteins. J. Virol. **74:**3623–3633.
6. **Deltenre, P., J. Henrion, V. Canva, S. Dharancy, F. Texier, A. Louvet, S. De Maeght, J. C. Paris, and P. Mathurin.** 2004. Evaluation of amantadine in chronic hepatitis C: a meta-analysis. J. Hepatol. **41:**462–473.
7. **Duff, K. C., P. J. Gilchrist, A. M. Saxena, and J. P. Bradshaw.** 1994. Neutron diffraction reveals the site of amantadine blockade in the influenza A M2 ion channel. Virology **202:**287–293.
8. **Engler, A., T. Stangler, and D. Willbold.** 2002. Structure of human immunodeficiency virus type 1 Vpr(34–51) peptide in micelle containing aqueous solution. Eur. J. Biochem. **269:**3264–3269.
9. **Galloux, M., S. Libersou, N. Morellet, S. Bouaziz, B. Da Costa, M. Ouldali, J. Lepault, and B. Delmas.** 2007. Infectious bursal disease virus, a non-enveloped virus, possesses a capsid-associated peptide that deforms and perforates biological membranes. J. Biol. Chem. **282:**20774–20784.
10. **Gandhi, C. S., K. Shuck, J. D. Lear, G. R. Dieckmann, W. F. DeGrado, R. A. Lamb, and L. H. Pinto.** 1999. Cu(II) inhibition of the proton translocation machinery of the influenza A virus M2 protein. J. Biol. Chem. **274:**5474–5482.
11. **Griffin, S., D. Clarke, C. McCormick, D. Rowlands, and M. Harris.** 2005. Signal peptide cleavage and internal targeting signals direct the hepatitis C virus p7 protein to distinct intracellular membranes. J. Virol. **79:**15525–15536.
12. **Griffin, S., C. Stgelais, A. M. Owsianka, A. H. Patel, D. Rowlands, and M. Harris.** 2008. Genotype-dependent sensitivity of hepatitis C virus to inhibitors of the p7 ion channel. Hepatology **48:**1779–1790.
13. **Griffin, S. D., L. P. Beales, D. S. Clarke, O. Worsfold, S. D. Evans, J. Jaeger, M. P. Harris, and D. J. Rowlands.** 2003. The p7 protein of hepatitis C virus forms an ion channel that is blocked by the antiviral drug, amantadine. FEBS Lett. **535:**34–38.
14. **Griffin, S. D., R. Harvey, D. S. Clarke, W. S. Barclay, M. Harris, and D. J. Rowlands.** 2004. A conserved basic loop in hepatitis C virus p7 protein is required for amantadine-sensitive ion channel activity in mammalian cells but is dispensable for localization to mitochondria. J. Gen. Virol. **85:**451–461.
15. **Harada, T., N. Tautz, and H. J. Thiel.** 2000. E2-p7 region of the bovine viral diarrhea virus polyprotein: processing and functional studies. J. Virol. **74:**9498–9506.
16. **Isherwood, B. J., and A. H. Patel.** 2005. Analysis of the processing and transmembrane topology of the E2p7 protein of hepatitis C virus. J. Gen. Virol. **86:**667–676.
17. **Jing, X., C. Ma, Y. Ohigashi, F. A. Oliveira, T. S. Jardetzky, L. H. Pinto, and R. A. Lamb.** 2008. Functional studies indicate amantadine binds to the pore of the influenza A virus M2 proton-selective ion channel. Proc. Natl. Acad. Sci. USA **105:**10967–10972.
18. **Johnson, V. G., P. J. Nicholls, W. H. Habig, and R. J. Youle.** 1993. The role of proline 345 in diphtheria toxin translocation. J. Biol. Chem. **268:**3514–3519.
19. **Jones, C. T., C. L. Murray, D. K. Eastman, J. Tassello, and C. M. Rice.** 2007. Hepatitis C virus p7 and NS2 proteins are essential for production of infectious virus. J. Virol. **81:**8374–8383.
20. **Kato, T., T. Date, M. Miyamoto, A. Furusaka, K. Tokushige, M. Mizokami, and T. Wakita.** 2003. Efficient replication of the genotype 2a hepatitis C virus subgenomic replicon. Gastroenterology **125:**1808–1817.
21. **Lindenbach, B. D., M. J. Evans, A. J. Syder, B. Wolk, T. L. Tellinghuisen, C. C. Liu, T. Maruyama, R. O. Hynes, D. R. Burton, J. A. McKeating, and C. M. Rice.** 2005. Complete replication of hepatitis C virus in cell culture. Science **309:**623–626.
22. **Meshkat, Z., M. Audsley, C. Beyer, E. J. Gowans, and G. Haqshenas.** 2009. Reverse genetic analysis of a putative, influenza virus M2 HXXXW-like motif in the p7 protein of hepatitis C virus. J. Viral Hepat. **16:**187–194.
23. **Moradpour, D., F. Penin, and C. M. Rice.** 2007. Replication of hepatitis C virus. Nat. Rev. Microbiol. **5:**453–463.
24. **Okada, A., T. Miura, and H. Takeuchi.** 2001. Protonation of histidine and

histidine-tryptophan interaction in the activation of the M2 ion channel from influenza a virus. Biochemistry **40:**6053–6060.
25. **Patargias, G., N. Zitzmann, R. Dwek, and W. B. Fischer.** 2006. Protein-protein interactions: modeling the hepatitis C virus ion channel p7. J. Med. Chem. **49:**648–655.
26. **Pavlovic, D., D. C. Neville, O. Argaud, B. Blumberg, R. A. Dwek, W. B. Fischer, and N. Zitzmann.** 2003. The hepatitis C virus p7 protein forms an ion channel that is inhibited by long-alkyl-chain iminosugar derivatives. Proc. Natl. Acad. Sci. USA **100:**6104–6108.
27. **Pawlotsky, J. M.** 2006. Therapy of hepatitis C: from empiricism to eradication. Hepatology **43:**S207-20.
28. **Perez-Berna, A. J., J. Guillen, M. R. Moreno, A. Bernabeu, G. Pabst, P. Laggner, and J. Villalain.** 2008. Identification of the membrane-active regions of hepatitis C virus p7 protein: biophysical characterization of the loop region. J. Biol. Chem. **283:**8089–8101.
29. **Pielak, R. M., J. R. Schnell, and J. J. Chou.** 2009. Mechanism of drug inhibition and drug resistance of influenza A M2 channel. Proc. Natl. Acad. Sci. USA **106:**7379–7384.
30. **Pinto, L. H., G. R. Dieckmann, C. S. Gandhi, C. G. Papworth, J. Braman, M. A. Shaughnessy, J. D. Lear, R. A. Lamb, and W. F. DeGrado.** 1997. A functionally defined model for the M2 proton channel of influenza A virus suggests a mechanism for its ion selectivity. Proc. Natl. Acad. Sci. USA **94:**11301–11306.
31. **Premkumar, A., L. Wilson, G. D. Ewart, and P. W. Gage.** 2004. Cation-selective ion channels formed by p7 of hepatitis C virus are blocked by hexamethylene amiloride. FEBS Lett. **557:**99–103.
32. **Sakai, A., M. S. Claire, K. Faulk, S. Govindarajan, S. U. Emerson, R. H. Purcell, and J. Bukh.** 2003. The p7 polypeptide of hepatitis C virus is critical for infectivity and contains functionally important genotype-specific sequences. Proc. Natl. Acad. Sci. USA **100:**11646–11651.
33. **Schnell, J. R., and J. J. Chou.** 2008. Structure and mechanism of the M2 proton channel of influenza A virus. Nature **451:**591–595.
34. **Steinmann, E., F. Penin, S. Kallis, A. H. Patel, R. Bartenschlager, and T. Pietschmann.** 2007. Hepatitis C virus p7 protein is crucial for assembly and release of infectious virions. PLoS Pathog. **3:**e103.
35. **Steinmann, E., T. Whitfield, S. Kallis, R. A. Dwek, N. Zitzmann, T. Pietschmann, and R. Bartenschlager.** 2007. Antiviral effects of amantadine and iminosugar derivatives against hepatitis C virus. Hepatology **46:**330–338.
36. **StGelais, C., T. J. Tuthill, D. S. Clarke, D. J. Rowlands, M. Harris, and S. Griffin.** 2007. Inhibition of hepatitis C virus p7 membrane channels in a liposome-based assay system. Antiviral Res. **76:**48–58.
37. **Stouffer, A. L., R. Acharya, D. Salom, A. S. Levine, L. Di Costanzo, C. S. Soto, V. Tereshko, V. Nanda, S. Stayrook, and W. F. DeGrado.** 2008. Structural basis for the function and inhibition of an influenza virus proton channel. Nature **451:**596–599.
38. **Takikawa, S., R. E. Engle, S. U. Emerson, R. H. Purcell, M. St Claire, and J. Bukh.** 2006. Functional analyses of GB virus B p13 protein: development of a recombinant GB virus B hepatitis virus with a p7 protein. Proc. Natl. Acad. Sci. USA **103:**3345–3350.
39. **Tang, Y., F. Zaitseva, R. A. Lamb, and L. H. Pinto.** 2002. The gate of the influenza virus M2 proton channel is formed by a single tryptophan residue. J. Biol. Chem. **277:**39880–39886.
40. **Wakita, T., T. Pietschmann, T. Kato, T. Date, M. Miyamoto, Z. Zhao, K. Murthy, A. Habermann, H. G. Krausslich, M. Mizokami, R. Bartenschlager, and T. J. Liang.** 2005. Production of infectious hepatitis C virus in tissue culture from a cloned viral genome. Nat. Med. **11:**791–796.
41. **Wang, C., R. A. Lamb, and L. H. Pinto.** 1995. Activation of the M2 ion channel of influenza virus: a role for the transmembrane domain histidine residue. Biophys. J. **69:**1363–1371.
42. **Xie, J., J. Zhao, P. B. Davis, and J. Ma.** 2000. Conformation, independent of charge, in the R domain affects cystic fibrosis transmembrane conductance regulator channel openings. Biophys. J. **78:**1293–1305.
43. **Yanagi, M., M. St. Claire, M. Shapiro, S. U. Emerson, R. H. Purcell, and J. Bukh.** 1998. Transcripts of a chimeric cDNA clone of hepatitis C virus genotype 1b are infectious in vivo. Virology **244:**161–172.
44. **Zhong, H., J. Lai, and K. W. Yau.** 2003. Selective heteromeric assembly of cyclic nucleotide-gated channels. Proc. Natl. Acad. Sci. USA **100:**5509–5513.
45. **Zhong, J., P. Gastaminza, G. Cheng, S. Kapadia, T. Kato, D. R. Burton, S. F. Wieland, S. L. Uprichard, T. Wakita, and F. V. Chisari.** 2005. Robust hepatitis C virus infection in vitro. Proc. Natl. Acad. Sci. USA **102:**9294–9299.